AMPTIAC

# LOCAL PLASTIC STRESSES IN SHEET ALUMINUM-ALLOY SPECIMENS WITH STRESS-CONCENTRATION FACTOR OF 2 UNDER CONSTANT-AMPLITUDE LOADING

*by John H. Crews, Jr.*

*Langley Research Center*
*Langley Station, Hampton, Va.*

20020319 117

# LOCAL PLASTIC STRESSES IN SHEET ALUMINUM-ALLOY SPECIMENS

## WITH STRESS-CONCENTRATION FACTOR OF 2

## UNDER CONSTANT-AMPLITUDE LOADING

By John H. Crews, Jr.

Langley Research Center
Langley Station, Hampton, Va.

NATIONAL AERONAUTICS AND SPACE ADMINISTRATION

# LOCAL PLASTIC STRESSES IN SHEET ALUMINUM-ALLOY SPECIMENS

## WITH STRESS-CONCENTRATION FACTOR OF 2

## UNDER CONSTANT-AMPLITUDE LOADING*

By John H. Crews, Jr.
Langley Research Center

## SUMMARY

Cyclic plastic stresses at notch roots in specimens under constant-amplitude repeated tension and reversed loading have been studied experimentally. The applied loads were cycled in edge-notched 2024-T3 aluminum-alloy sheet specimens, which had a stress-concentration factor of 2, until local stress conditions stabilized. Determination of local stress histories was made by recording local strain histories during cycling and reproducing these histories in simple unnotched specimens. The fatigue lives for the notched specimens were estimated from the stabilized local stresses and fatigue data for the unnotched specimens. These estimations compared favorably with fatigue-life data for the notch configuration tested.

In addition, an expression for calculating local first-cycle plastic stresses is presented. An acceptable correlation is shown between predicted stresses and experimental data within the scope of the investigation.

## INTRODUCTION

Fatigue failures in structures characteristically originate at geometric discontinuities that produce local stresses higher than the nominal stresses applied. In applications that are critical to excessive weight, these local stresses are frequently in the plastic range and as a result are accompanied by residual stresses. An understanding of the influence of cyclic plastic action on local stresses should lead to the development of methods for estimating fatigue behavior of bodies containing stress raisers.

Because of the inherent history dependence of cyclic plastic stresses, the task of analyzing these stresses at a notch is very complex and consequently, the problem has received little attention in the literature.

---

*This paper is based in part on a paper entitled, "A Study of Cyclic Plastic Stresses at a Notch Root" by J. H. Crews, Jr., and H. F. Hardrath presented at the SESA (Society for Experimental Stress Analysis) Spring Meeting, Denver, Colorado, May 5-7, 1965.

L-4610

The present investigation was undertaken as a starting point for relating the local plastic stresses to applied loads. Local plastic conditions in notched specimens were studied experimentally under constant-amplitude loading for a single material and one specimen configuration. Preliminary methods were developed for calculating local stresses during the first loading cycle and for estimating fatigue lives from stabilized local stresses. Further study is expected to lead to the development of such methods to include other specimen shapes and materials and for variable-amplitude loading.

## SYMBOLS

The units used for the physical quantities defined in this paper are given both in U.S. Customary Units and in the International System of Units (SI) (ref. 1). Appendix A presents factors relating these two systems of units.

$E$         Young's modulus, psi $(N/m^2)$

$E_S$        secant modulus corresponding to local stress at notch root for monotonically increasing tensile loads (in first cycle), psi $(N/m^2)$

$E_S'$       secant modulus corresponding to local stress at notch root for negative loading from tension (in first cycle), psi $(N/m^2)$

$E_S''$      secant modulus corresponding to local stress at notch root for positive loading from compression (in first cycle), psi $(N/m^2)$

$K_{el}$      experimental elastic stress-concentration factor

$K_p$      plastic stress-concentration factor for monotonically increasing tensile loads

$K_p'$      plastic stress-concentration factor for negative loading from tension (in first cycle)

$K_p''$     plastic stress-concentration factor for positive loading from compression (in first cycle)

$K_T$      theoretical elastic stress-concentration factor

$N$       number of cycles

$R$       ratio of $S_{min}/S_{max}$

$S$       nominal net-section stress, ksi $(MN/m^2)$

$\Delta S$      nominal stress range, ksi $(MN/m^2)$

$t$       specimen thickness, inches (cm)

$\epsilon$       local strain at notch root

$\rho$      notch-root radius, inches (cm)

$\sigma$      local stress at notch root, ksi $(MN/m^2)$

$\sigma_r$      local residual stress at notch root, ksi $(MN/m^2)$

$\sigma_y$      tensile yield stress (0.2-percent offset), ksi $(MN/m^2)$

Subscripts:

max      maximum

min      minimum

## EXPERIMENTAL PROCEDURE

### Specimens

Edge-notched sheet specimens of 2024-T3 aluminum alloy were used for all tests in this study. The notched specimen configuration and the companion tensile specimen are shown in figure 1. Dimensions of the notched specimen were selected for an elastic stress-concentration of 2 (ref. 2) and for a large ratio of notch radius to a gage length over which local strain measurements were feasible. Each pair of notched and tensile specimens was machined from adjacent sheet material to minimize the effects of variations in material characteristics within the sheet, and all specimens were oriented parallel to the grain direction of the sheet stock. In an attempt to minimize machining stresses, sharp tools were used and only 0.003 inch (80 $\mu$m) of material was removed during the final step in preparing the notches.

### Companion Specimen Method

Local stress histories at the notch root were determined by a companion specimen method. The basis of this method is that stress and strain will always be related in a similar manner for a given state of stress, stress or strain history, and material. For each loading sequence strain histories were measured at the notch roots, where the state of stress is uniaxial. These strain histories were reproduced under uniaxial tension in unnotched companion specimens to determine the corresponding stresses. The sequence of stresses found in this manner was the local stress history for the notch root.

### Instrumentation

Both photoelastic coatings and resistance strain gages were used for strain measurements during the test program. For the photoelastic method, birefringent coatings were bonded to the flat surfaces of the specimen near the notches, and fringe orders at the edge of the notch roots were observed with a small-field reflective polariscope

Material: 2024-T3
$K_T = 2.0$
$t = 0.162"(0.41\,cm)$
$\rho = 1.672"(4.25\,cm)$

11.90"
(30.23 cm)

35"
(89 cm)

7.84"
(19.9 cm)

17.5"
(44.5 cm)

Photoelastic coatings
Strain gages

(Both notches
instrumented)

0.800"
(2.03 cm)

12" (30.5 cm)

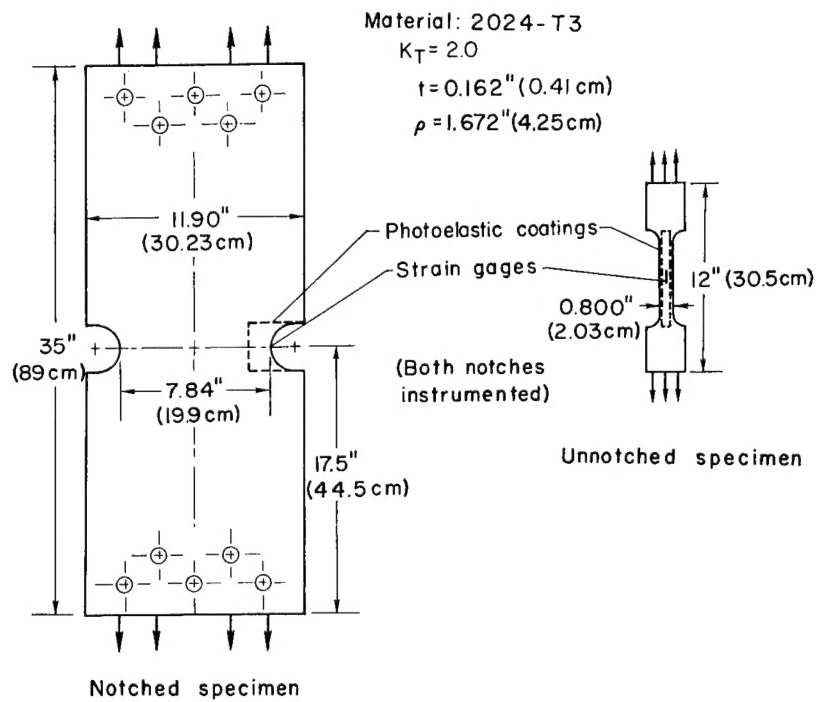Unnotched specimen

Notched specimen

Figure 1.- Specimen dimensions and instrumentation.

during load cycling. The fringe order histories were then reproduced in unnotched specimens clad with similar birefringent material to find the local stress histories. This method required extremely tedious observations and was subject to errors due to edge effects and fringe fadeout at high strain levels. In addition, variations in Poisson's ratio with plastic deformation precluded the calculation of cyclic normal strains from fringe order readings. As a result, to determine local strains, a traversing microscope was employed to take gage length measurements on the unnotched specimens while they were being loaded to reproduce the fringe histories. The photoelastic method was abandoned because of its time-consuming procedure and the fringe fadeout difficulties.

Foil strain gages, bonded in the notch root, proved to be more convenient and were used for most tests. A small gage length (1/16 inch (0.16 cm)) was selected to reduce the effects of the strain gradient within the gage length. In addition, the two gages, one at each notch, were connected in series to indicate the average notch-root strain. A null-balance strain indicator employing a Wheatstone bridge was used.

Changes in strain-gage characteristics with cycling have been noted (ref. 3) but were not believed to affect the stress results in this study. A comparison of strain-gage measurements with those of the traversing-microscope method indicated only small errors in strain-gage performance for the first cycle of loading; however, with subsequent cycling, larger changes were observed. Nevertheless, for the companion method these strain-gage measurements may be considered as only "transfer" values relating unnotched specimen stresses to the cyclic loading of the notched specimen. Therefore, if similar gages are used on both the notched and unnotched specimens, gage errors due to cyclic straining, which are characteristic of the given gage type, should not result in significant errors in the local stress data.

Specimen Loading

The notched specimens were cycled under repeated tension (R = 0) and completely reversed (R = -1) constant-amplitude loading. Nominal stresses (net section) were used over the range from that corresponding to incipient local yielding to that approaching the yield stress on the net section. For each test, cycling was continued until local stresses stabilized.

A 120 000-pound-capacity (534 kN) double-acting hydraulic jack was used for loading the notched specimens. A lower range of this jack, 12 000-pound (53 kN), was used for most of the unnotched specimens. For three unnotched tests at 40, 45, and 50 ksi (276, 310, and 344 MN/m$^2$) nominally stressed with reversed loading, a 20 000-pound (89 kN) servo-controlled, hydraulic test machine was used. For both the notched and the companion tests, guide plates similar to those described in reference 4 were used to prevent buckling during compressive loadings.

# RESULTS AND DISCUSSION

## General

For this study, stress-concentration factor is defined as the ratio of local stress at the notch root to the average stress on the net section. Experimental elastic stress-concentration factors have been obtained from tensile loading data prior to local yielding and are given in tables I and II. These experimental values exceed the value of 2.0 from Neuber theory (ref. 2) by approximately 5 percent.

In this investigation only stresses at the notch root were studied, and all references to local stress conditions are confined to behavior at this point. The general behavior at this critical point is illustrated in figure 2 for cyclic loading. For the first cycle of repeated loading (R = 0), a typical local behavior is described by the path OAB; where A represents the maximum local stress and strain and B represents the compressive residual stress and strain occurring upon unloading. For completely reversed loading (R = -1), a typical set of local stress-strain conditions is described by OABCD, where C represents the minimum local stress and strain, and D represents the tensile residual
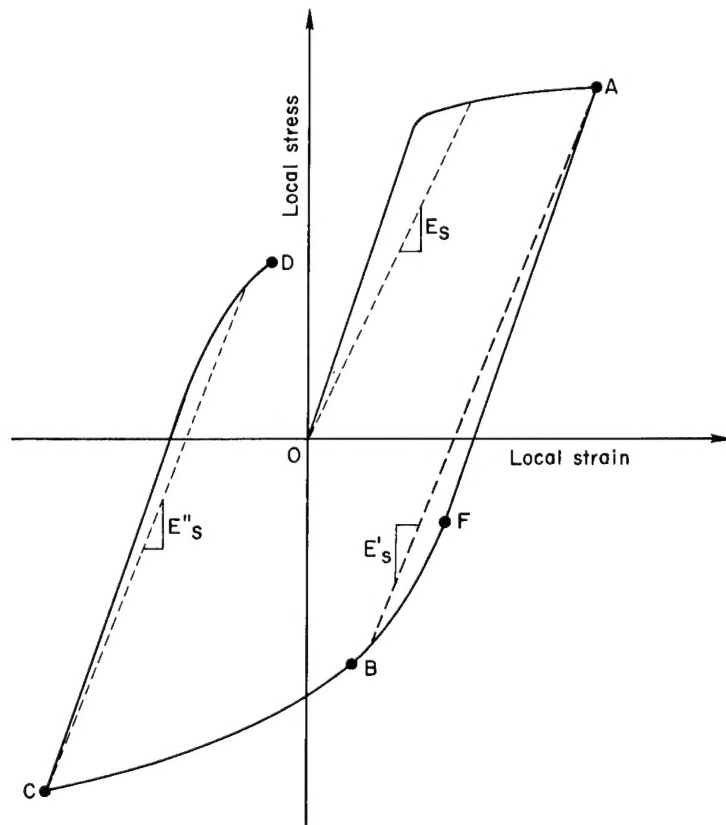


Figure 2.- Local stress-strain curve for first cycle of loading.

stress and strain at the end of the first full cycle. The secant moduli shown in this figure will be explained later.

Results of this study are summarized in tables I and II and are discussed in the following sections. In addition, the tables include identification of the strain-measuring technique employed for each test. Both techniques gave similar results.

Repeated Loading

Figure 3 illustrates local stress-strain data for the first cycle of repeated loading (R = 0) for six values of maximum nominal stress. The unloading in each case produced a compressive residual stress. For tests with moderate nominal stresses the residual stresses appeared to be elastic. However, in tests at higher nominal stresses
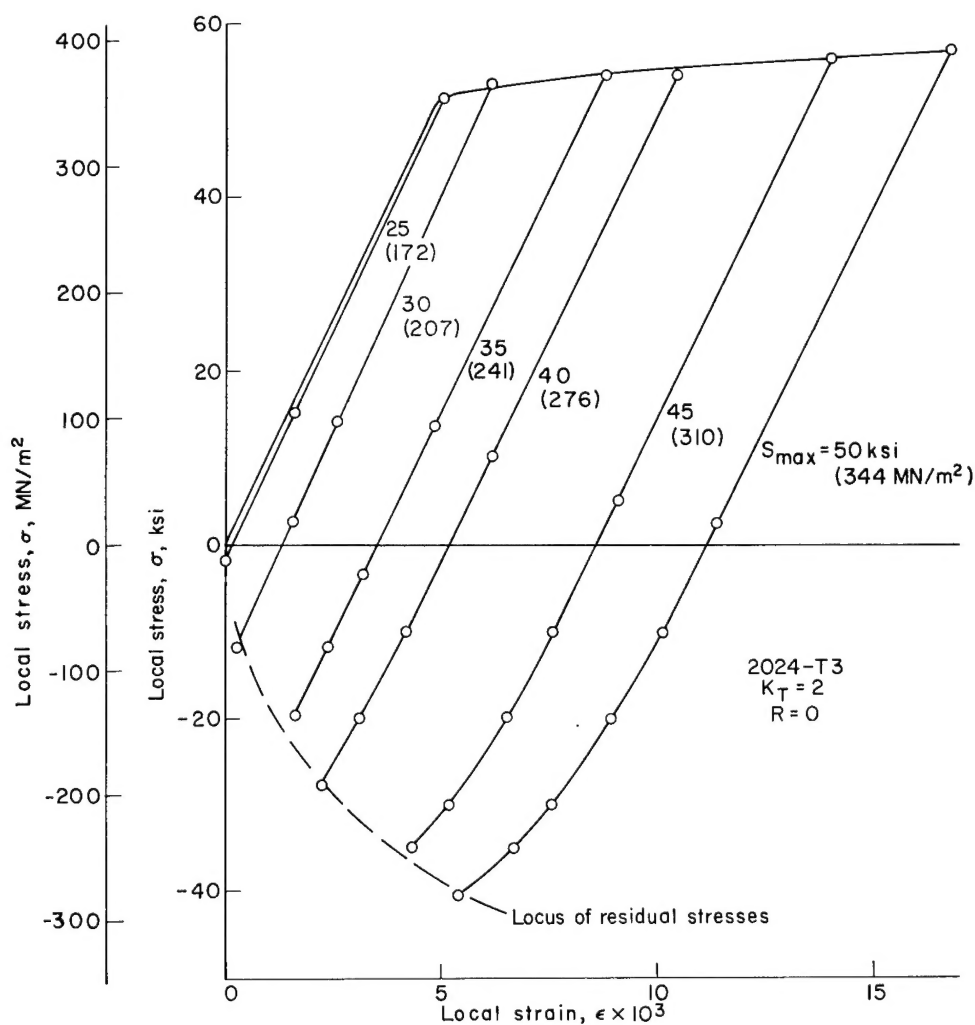


Figure 3.- Local stress-strain curves for first cycle repeated loading (R = 0).

$\left(S \gtrsim 0.8\sigma_y\right)$, local yielding occurred. The locus of these compressive residual stresses as influenced by nominal stress is shown by the dashed line.

Maximum and residual local stresses measured during each of several cycles of repeated constant-amplitude loading are shown in figure 4. The three pairs of curves represent typical histories of maximum stress and of compressive residual stress for three different levels of nominal stress. A small reduction in maximum local stresses was observed during the first few cycles with a corresponding increase in compressive residual stresses. Thus, the local mean stress decreased somewhat while the local stress range remained virtually unchanged during these cycles. Beyond the tenth
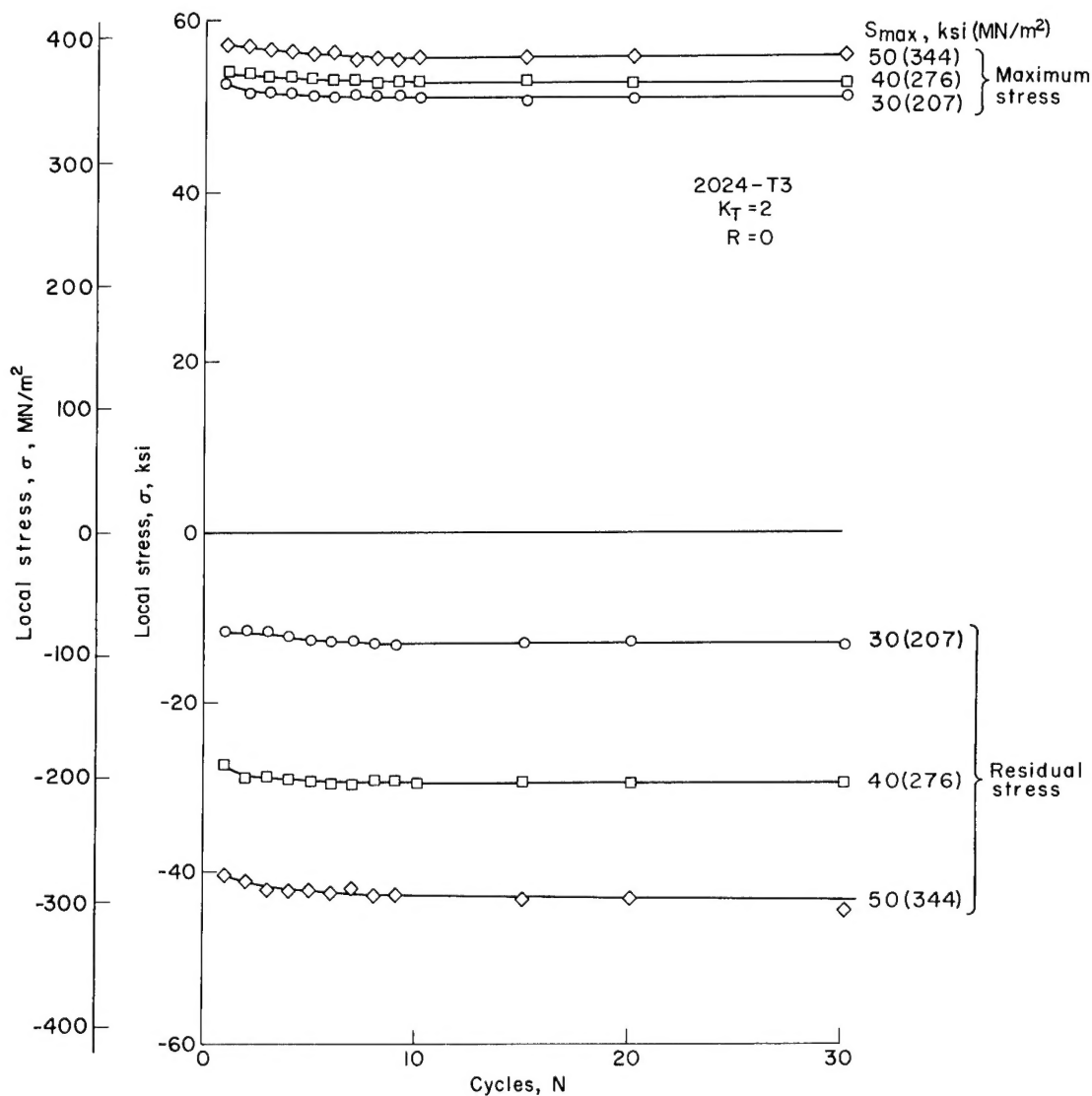


Figure 4.- Stabilization of local stresses for repeated constant-amplitude loading (R = 0).

cycle, local stresses returned to essentially the same values in each cycle. These local stabilized stresses and those presented in table I for the other tests are used later in estimating fatigue life for this specimen configuration.

⌈ Reversed Loading ⌋                                    *to p. 17*

The local stress-strain histories measured during the first cycle in each of several tests with completely reversed loadings are presented in figure 5. For these tests four characteristic values of local stress are of interest: the maximum, the residual after unloading (half cycle), the minimum, and the residual after completing the cycle
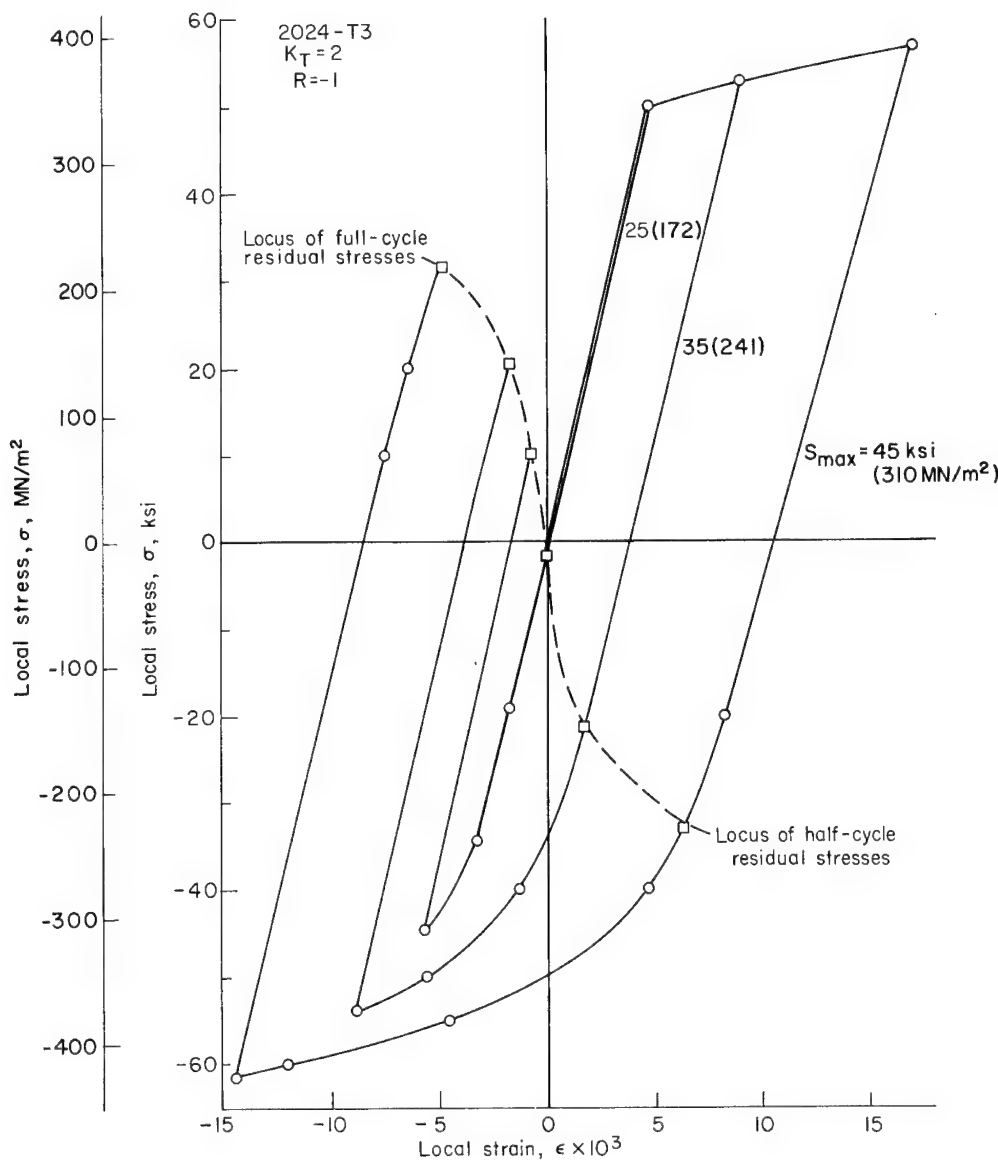


Figure 5.- Local stress-strain curves for first cycle of reversed loading (R = -1).

9

(full cycle). The loci of the residual stresses as influenced by the nominal stress are shown as dashed lines. As was the case with tests at R = 0, the residual stresses are subject to some plastic action for tests in which high nominal stresses were applied. The half-cycle and full-cycle values of residual stress for a given load level were approximately symmetrical about zero except for the test of S = 25 ksi $\left(172 \text{ MN/m}^2\right)$.

Typical histories of these four characteristic stresses during subsequent cycles of reversed loading are presented in figure 6. The absolute values of maximum and minimum stresses increased appreciably and thus increased the local stress range during each of the first 15 to 20 cycles, after which the stress range remained stable. Similarly, the absolute values of residual stress decreased during each of these cycles and then stabilized. The stabilized values of maximum and minimum stresses were approximately symmetric about zero. Local stresses for the reversed loading tests are presented in table II.

## Fatigue Estimates

The stabilized values of local stress described in the previous section were used to estimate the fatigue lives of similar notched specimens tested at the same nominal
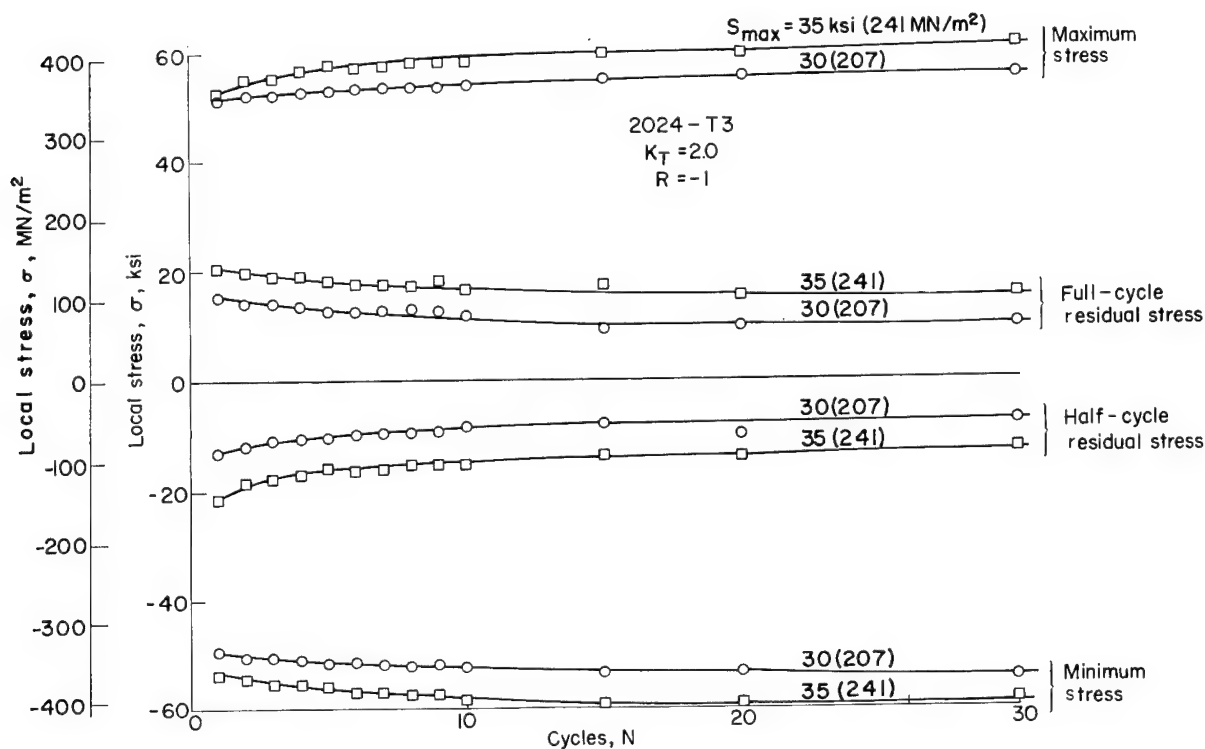


Figure 6.- Local stress stabilization for reversed constant-amplitude loading (R = -1).

10

stress levels. The fatigue data used for the comparisons were for edge-notched 2024-T3 aluminum-alloy sheet specimens with $K_T = 2$ and subjected to constant-amplitude axial loads with $R = 0$ and $R = -1$ (refs. 5 and 6).

The lives were obtained on the assumption that failure would occur in the notched specimen in the same number of cycles that produced failure in unnotched specimens subjected to the repeated stresses equal to the local stabilized stresses observed in the present tests. The life estimates were taken from fatigue data for tests of unnotched specimens of the same material (ref. 4).

The resulting estimates of life and fatigue data are listed in table III and are plotted in figure 7. All the life estimates agree with the data within a factor of approximately 2. This correlation is encouraging as it offers the hope that fatigue lives of notched parts can be estimated from behavior of unnotched specimens provided the effects of notches and plastic action can be established. Unfortunately, the key information needed to accomplish the estimate is the relation between the applied nominal stresses and the sta-bilized local stresses. To this point, this relationship is obtainable only by rather
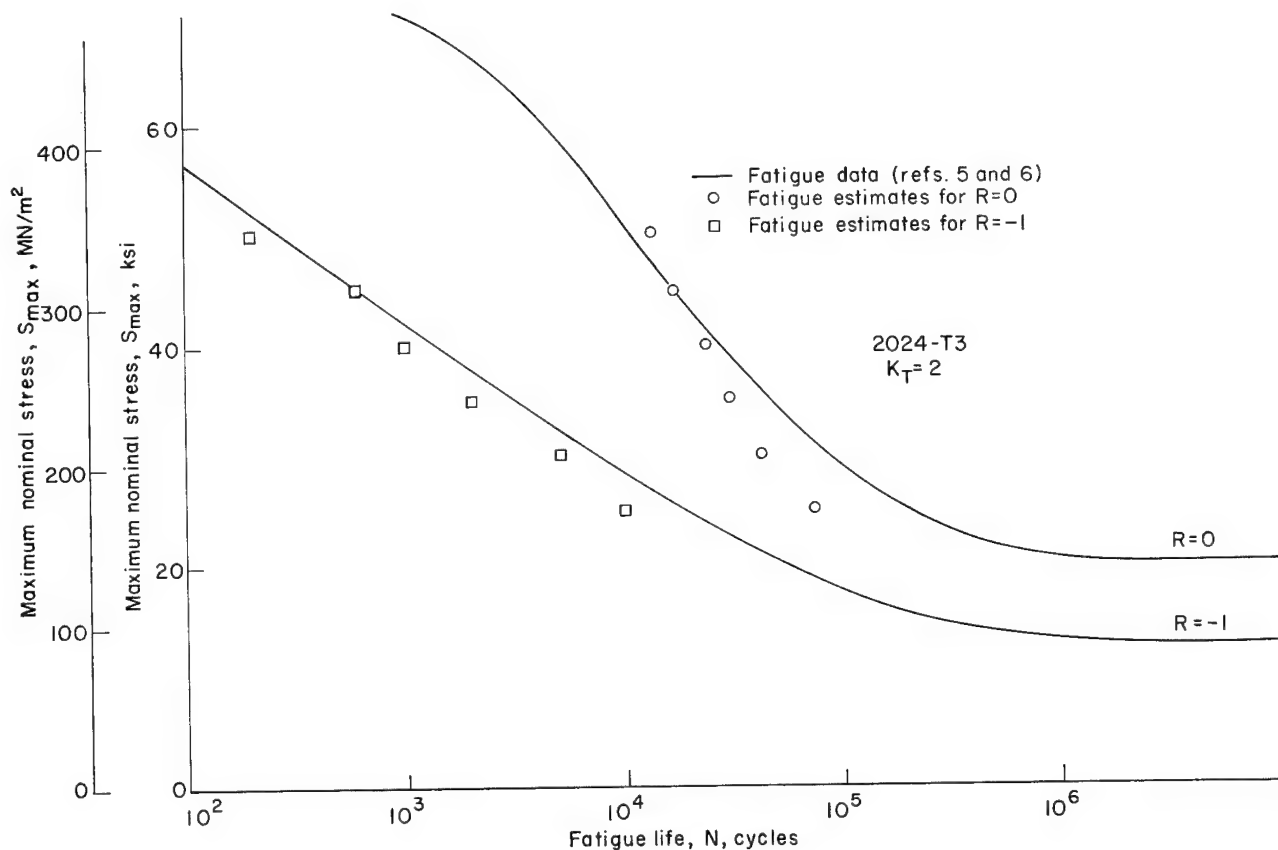


Figure 7.- Fatigue predictions.

painstaking tests. As an initial step, the following section presents a preliminary method for computing the desired local stresses for the first cycle of loading.

## LOCAL STRESS CALCULATIONS

### Proposed Method

Previous studies of stress-concentration factors as modified by plastic action have been conducted at the NASA Langley Research Center. (See refs. 7 and 8.) Briefly, these studies have led to the development of the following generalized formula:

$$\sigma = SK_p = S\left[1 + \left(K_T - 1\right)\right]\frac{E_s}{E} \tag{1}$$

This relation yields, within engineering accuracy, estimates of local plastic stresses for arbitrary stress raisers under monotonically increasing loads provided $S < \sigma_y$, at least for small plastic strains (up to 1 or 2 percent). The stress A in figure 2 is calculable by a trial-and-error solution of equation (1).

For unloading from point A, an additional term must be added to equation (1). The basic approach in developing this term can be easily understood if unloading from point A is considered as a negative application of loading. From this viewpoint, point A would be the "origin" of the unloading path AC. It then follows that, for any level of negative load, the local stress relative to point A might be found by the use of an appropriate stress-concentration factor in a manner analogous to the use of $K_p$ for the tensile range OA. This approach was used in the following development. Attention is restricted first to residual stresses after unloading and then broadened to include the entire stress range AC.

In cases where no plastic yielding occurs during the negative loading, the desired stress-concentration factor is $K_T$. For an unloaded specimen, the residual stress F in figure 2 is calculated from the equations

$$\left.\begin{array}{l} \sigma_r = \sigma_{max} - S_{max}K_T \\[2ex] \sigma_r = S_{max}\left(K_p - K_T\right) \end{array}\right\} \tag{2}$$

However, if local compressive yielding occurs, $K_T$ no longer applies and a plasticity correction is required. It is proposed that this plasticity correction be obtained by a method involving secant moduli similar to that employed for equation (1). A typical secant modulus $E_s'$ required for this calculation is shown in figure 2. It has its origin

12

at point A, the point at which unloading began. The following relation is proposed for cal-
culating compressive residual stresses in the plastic range:

$$\sigma_r = S_{max}\left(K_p - K_p'\right) \tag{3}$$

where $K_p'$ is the plastic stress-concentration factor for negative loading (unloading)

$$K_p' = 1 + \left(K_T - 1\right)\frac{E_s'}{E}$$

The range of applicability of equation (3) may be readily extended to solve the gen-
eral case of any negative loading from tension that results in compressive yielding:

$$\sigma = S_{max}K_p - \left(S_{max} - S\right)K_p' \tag{4}$$

where $S$ is the nominal stress for which $\sigma$ is sought.

This relation is a generalization of the three preceding expressions and is applicable
for the full range of local stress represented by OABC in figure 2.

If the procedure of unloading from point A to established $E_s'$ values is repeated
for positive loading from point C in figure 2, the appropriate secant modulus $E_s''$ may
also be found for the third excursion into the plastic range. The addition of another term
to equation (4) leads to an expression for the local behavior during this fourth quarter
cycle of loading:

$$\sigma = S_{max}K_p - \left(S_{max} - S_{min}\right)K_p' - \left(S_{min} - S\right)K_p'' \tag{5}$$

where $K_p''$ is the plastic stress-concentration factor for the third excursion into the
plastic range

$$K_p'' = 1 + \left(K_T\right) - 1\frac{E_s''}{E}$$

where $E_s''$ is the appropriate secant modulus referenced to the minimum local stress
experienced (C in fig. 2).

Solutions for these equations require a trial-and-error procedure similar to that
used to solve equation (1). In principle, stress-strain curves OA, AC, and CD are
required for the calculations of A, C, and D, respectively. An unnotched specimen must
be loaded into tension to point A, loaded in compression to point C, and finally loaded in
tension to point D to generate a curve similar to that in figure 2. Since the calculated

stresses corresponding to A and C are functions of the stress-strain curve being gener-
ated, trial-and-error calculations are required during the test. A less tedious but more
lengthy procedure would involve three separate tests, one for each excursion into the
plastic range, to determine OA, OAC, and OACD. Approximations are introduced in the
following section which simplify this procedure.

## Comparison With Data

For each level of nominal stress, a simple unnotched specimen was loaded in a
manner such that the notch strain history was reproduced, as previously explained.
Therefore, for each test a stress-strain curve similar to that of figure 2 was obtained for
the first cycle. The segments of each curve corresponding to OA were found to be gen-
erally similar and a faired stress-strain curve was used in establishing values of $E_S$.
In addition, the segments corresponding to AC for each test were also found to have
essentially equal elastic ranges and consistent shapes for the early stages of the plastic
range. Therefore, as a simplifying approximation a single faired curve was also used to
determine values of $E_S'$. The curves of $K_p$ and $K_p'$ shown in figure 8 were calcu-
lated for the full range of nominal stresses with the aid of these faired stress-strain
curves.

The similar shapes of the local stress-strain curves for unloading from A and
unloading from C suggest another simplifying assumption. The assumption made is that
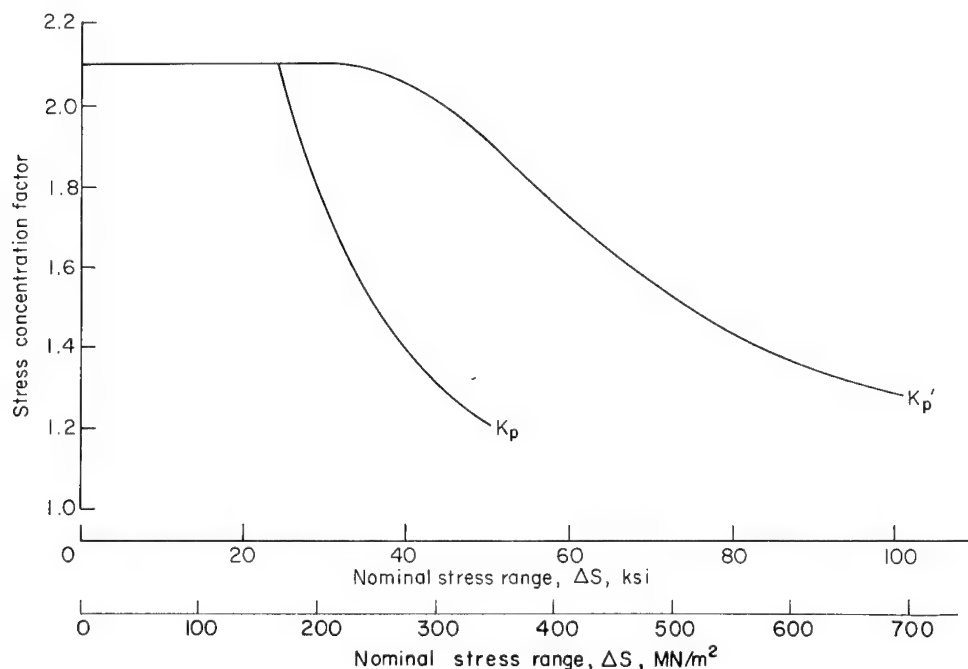


Figure 8.- Plastic stress concentration factors.

14

the segment CD, of the stress-strain curve in figure 2, has the same shape as the segment AB. Thus, the curve for $K_p'$ in figure 8 may be used to determine the $K_p''$ in equation (5). However, $K_p'$ and $K_p''$ must be evaluated independently for the particular nominal stress range over which each acts. These separate evaluations preclude the combination of $K_p'$ and $K_p''$ terms in equation (5).

Equation (4) was used with the curves of $K_p$ and $K_p'$ to calculate first-cycle local stresses for repeated loading (R = 0). The maximum local stresses were calculated by setting $S = S_{max}$ in this generalized equation, thus reducing it to equation (1). The compressive residual stresses at the end of the first full loading cycle were found by setting $S = 0$. With this substitution, the generalized equation reduces to equation (3). These calculated stresses are compared in figure 9 with the first-cycle test data in the range investigated. For a point-by-point comparison, data and calculated results are also presented in table I.
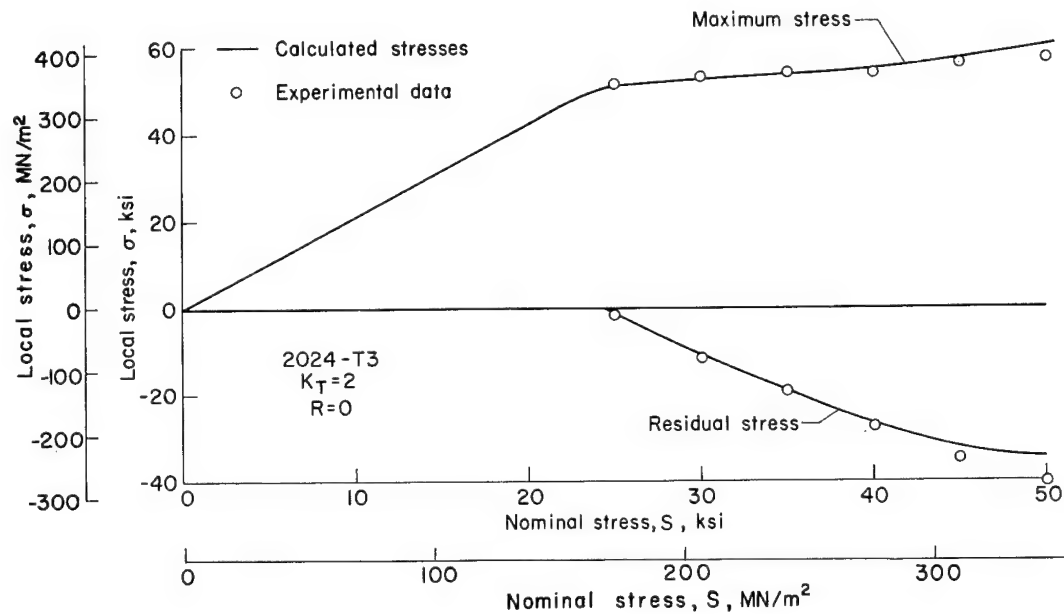


Figure 9.- First-cycle stresses for repeated loading.

An acceptable correlation between calculation and experiment is observed in figure 9. The minor discrepancies for the high stress level tests are probably attributable to the use of the photoelastic-coating technique. Since the coating is bonded to only one side of the specimen, this method is subject to errors due to initial specimen warpage. Better correlation will be shown for these same stress levels in the following discussion of tests using strain gages.

For reversed loading (R = -1), equations (4) and (5) were used to calculate local stresses. Maximum local and compressive residual stresses were calculated as in the

preceding case of repeated loading from equation (4). Equation (4) was also used to calculate minimum local stresses by setting $S = S_{min}$. Equation (5) and the curve of $K_p'$ in figure 8 were used to calculate tensile residual stresses occurring at the end of a first cycle of completely reversed loading. These four characteristic stresses and the corresponding observed data are listed in table II and are shown in figure 10.

With the exception of tensile (full-cycle) residual stresses, good correlation is illustrated by figure 10 between calculated curves and test data. The assumption regarding the similarity in stress-strain curves for unloading from both tension and compression is partially responsible for the errors in predicted full-cycle stresses.
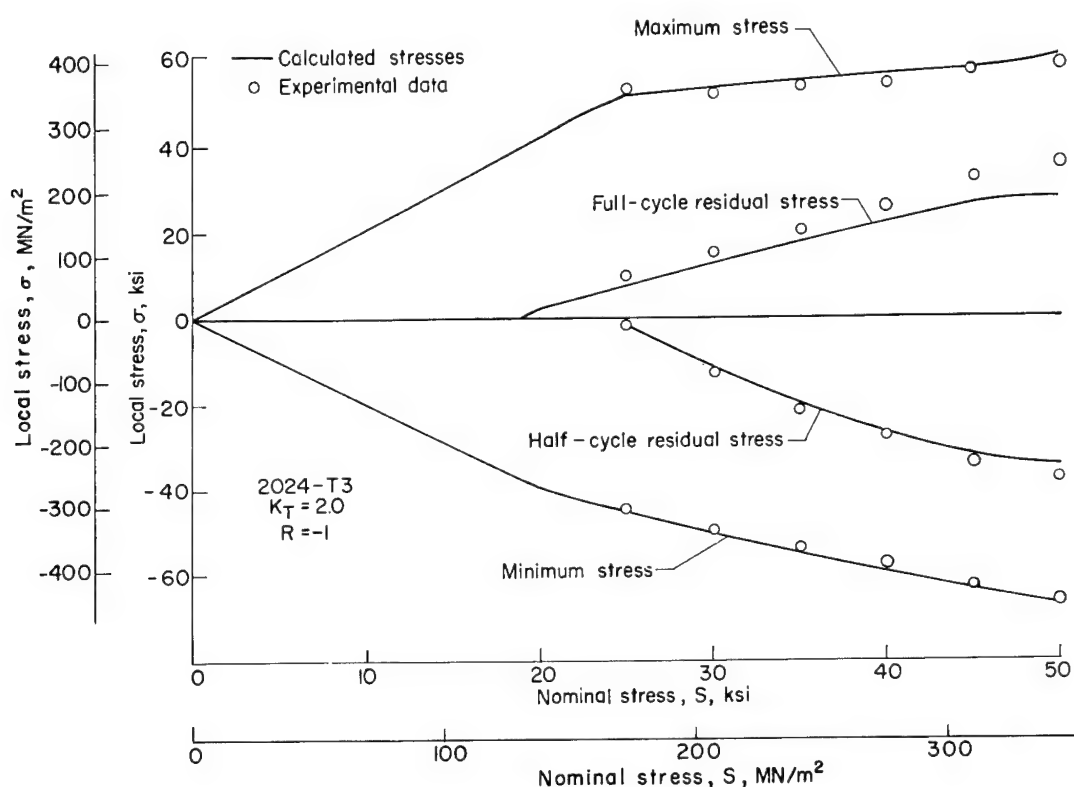


Figure 10.- First-cycle stresses for completely reversed loading.

Deviations of individual stress-strain curves from the faired curves used in calculating $K_p$ and $K_p'$ are expected to account for some discrepancies in all calculated stresses. Calculations and data based entirely on the behaviors of a given specimen and its companion specimen were found to be in very close agreement. In general, an acceptable correlation is displayed between the calculated results and the experimental data found in this study.

As demonstrated in this paper, estimates of stabilized stresses are useful in predicting fatigue lives of notched components. The equations presented herein, if found to

16

hold for arbitrary geometries and other materials in the first cycle of loading, will serve as an important step in calculating these stabilized conditions at a stress raiser. Further, the information regarding residual stresses obtained in this study should be useful for explaining some of the effects of loading sequence on cumulative damage as observed in variable-amplitude fatigue tests.

## CONCLUDING REMARKS

From this study of plastic stress histories at notch roots in edge-notched specimens of sheet 2024-T3 aluminum alloy under constant-amplitude load cycling, the following conclusions are made:

1. For the notch configuration tested which had an elastic stress-concentration factor of 2, local residual yielding occurs upon unloading from high nominal stresses (nominal net-section stress greater than 0.8 tensile yield stress).

2. Stabilization of local stresses occurred in less than 30 cycles.

3. For repeated loading, a small reduction in maximum local stress was observed during the first few cycles with a corresponding increase in the absolute value of compressive residual stress. Thus, the local mean stress decreased somewhat while the local stress range remained virtually unchanged.

4. Completely reversed load cycling resulted in appreciable increases in both maximum and minimum local stress magnitudes before stabilization occurred. Compressive residual stresses measured at the end of each half-cycle and tensile residual stresses measured at the end of each full cycle decreased significantly in magnitude before stabilizing.

5. Useful fatigue predictions were made for the notched specimens from stabilized local stress conditions and fatigue data for unnotched specimens of the same material.

6. The generalized notch-stress equation, presented in this paper, adequately described local plastic stress behavior for the first cycle of loading in these tests.

Langley Research Center,
    National Aeronautics and Space Administration,
        Langley Station, Hampton, Va., August 27, 1965.

## APPENDIX A

## CONVERSION OF U.S. CUSTOMARY UNITS TO SI UNITS

The International System of Units (SI) was adopted by the Eleventh General Conference on Weights and Measures, Paris, October 1960, in Resolution No. 12 (ref. 1). Conversion factors for the units used herein are given in the following table:

| Physical quantity | U.S. Customary Unit | Conversion factor (*) | SI Unit |
|---|---|---|---|
| Length . . . . . | in. | 0.0254 | meters (m) |
| Stress . . . . . | psi = lbf/in$^2$ | $6.895 \times 10^3$ | newtons per square meter $\left( n/m^2 \right)$ |
| Weight . . . . . | lbf | 4.448 | newton (N) |

*Multiply value given in U.S. Customary Unit by conversion factor to obtain equivalent value in SI Units.

Prefixes to indicate multiple of units are as follows:

| Prefix | Multiple |
|---|---|
| kilo (k) | $10^3$ |
| mega (M) | $10^6$ |
| centi (c) | $10^{-2}$ |
| micro ($\mu$) | $10^{-6}$ |

## REFERENCES

1. Mechtly, E. A.: The International System of Units — Physical Constants and Conversion Factors. NASA SP-7012, 1964.

2. Neuber, Heinz: Theory of Notch Stresses: Principles for Exact Calculation of Strength With Reference To Structural Form and Material. AEC-TR-4547, U.S. At. Energy Comm., 1961.

3. Wnuk, S. P., Jr.: Performance Characteristics of Bonded Strain Gages Under Repeated Cyclic Strain. Paper presented at SESA Annual Meeting (Cleveland, Ohio), Oct. 28-30, 1964.

4. Grover, H. J.; Hyler, W. S.; Kuhn, Paul; Landers, Charles B.; and Howell, F. M.: Axial-Load Fatigue Properties of 24S-T and 75S-T Aluminum Alloy as Determined in Several Laboratories. NACA Rept. 1190, 1954. (Supersedes NACA TN 2928.)

5. Illg, Walter: Fatigue Tests on Notched and Unnotched Sheet Specimens of 2024-T3 and 7075-T6 Aluminum Alloys and of SAE 4130 Steel With Special Consideration of the Life Range From 2 to 10,000 Cycles. NACA TN 3866, 1956.

6. Grover, H. J.; Bishop, S. M.; and Jackson, L. R.: Fatigue Strengths of Aircraft Materials. Axial-Load Fatigue Tests on Notched Sheet Specimens of 24S-T3 and 75S-T6 Aluminum Alloys and of SAE 4130 Steel With Stress-Concentration Factors of 2.0 and 4.0. NACA TN 2389, 1951.

7. Stowell, Elbridge Z.: Stress and Strain Concentration at a Circular Hole in an Infinite Plate. NACA TN 2073, 1950.

8. Hardrath, Herbert F.; and Ohman, Lachlan: A Study of Elastic and Plastic Stress Concentration Factors Due to Notches and Fillets in Flat Plates. NACA Rept. 1117, 1953. (Supersedes NACA TN 2566.)

TABLE I.- LOCAL STRESS DATA AND CALCULATED RESULTS FOR REPEATED LOADING (R = 0)

| Smax | | Experimental method (*) | $K_{el}$ | Maximum local stress | | | | | | Residual stress | | | | | |
|---|---|---|---|---|---|---|---|---|---|---|---|---|---|---|---|
| | | | | First cycle | | | | Stabilized | | First cycle | | | | Stabilized | |
| | | | | Experimental | | Calculated | | | | Experimental | | Calculated | | | |
| ksi | MN/m² | | | ksi | MN/m² | ksi | MN/m² | ksi | MN/m² | ksi | MN/m² | ksi | MN/m² | ksi | MN/m² |
| 25 | 172 | SG | 2.13 | 51.3 | 353 | 51.0 | 351 | 51.1 | 352 | -1.8 | -12.4 | -1.5 | -10.3 | -2.0 | -13.8 |
| 30 | 207 | PC | 2.14 | 53.0 | 365 | 52.2 | 360 | 51.0 | 351 | -11.7 | -80.6 | -10.8 | -74.4 | -13.0 | -89.6 |
| 35 | 241 | SG | 2.15 | 53.9 | 371 | 53.4 | 368 | 52.5 | 362 | -19.6 | -135 | -19.6 | -135 | -21.7 | -150 |
| 40 | 276 | PC | 2.04 | 53.9 | 371 | 55.4 | 382 | 52.8 | 364 | -27.7 | -191 | -26.6 | -183 | -29.8 | -205 |
| 45 | 310 | PC | 2.09 | 56.0 | 386 | 57.8 | 398 | 55.0 | 378 | -35.0 | -241 | -32.2 | -222 | -37.0 | -255 |
| 50 | 344 | PC | 2.09 | 57.0 | 393 | 60.5 | 417 | 55.5 | 382 | -40.4 | -278 | -34.4 | -237 | -43.0 | -296 |

*PC, photoelastic coating; SG, strain gage.

TABLE II.- LOCAL STRESS DATA AND CALCULATED RESULTS FOR REVERSED LOADING (R = -1)

(a) U.S. Customary Units

| $S_{max}$, ksi | Experimental method (*) | $K_{el}$ | Maximum local stress, ksi | | | Half-cycle residual stress, ksi | | | Minimum local stress, ksi | | | Full-cycle residual stress, ksi | | |
|---|---|---|---|---|---|---|---|---|---|---|---|---|---|---|
| | | | First cycle | | Stabilized | First cycle | | Stabilized | First cycle | | Stabilized | First cycle | | Stabilized |
| | | | Experimental | Calculated | | Experimental | Calculated | | Experimental | Calculated | | Experimental | Calculated | |
| 25 | SG | 2.16 | 52.4 | 51.0 | 53.5 | -1.5 | -1.5 | 0 | -44.7 | -44.5 | -45.5 | 10.2 | 8.0 | 9.2 |
| 30 | SG | 2.12 | 51.4 | 52.2 | 56.0 | -12.8 | -10.8 | -7.5 | -49.6 | -51.0 | -54.5 | 15.5 | 12.0 | 10.0 |
| 35 | SG | 2.15 | 52.9 | 53.4 | 61.0 | -21.4 | -19.6 | -12.5 | -53.8 | -55.4 | -59.5 | 20.9 | 17.6 | 15.0 |
| 40 | SG | 2.12 | 53.9 | 55.4 | 63.5 | -27.8 | -26.6 | -20.5 | -57.9 | -59.0 | -65.0 | 25.6 | 23.0 | 20.0 |
| 45 | SG | 2.17 | 56.7 | 57.8 | 64.5 | -34.1 | -32.2 | -29.0 | -62.6 | -63.7 | -68.0 | 32.2 | 26.3 | 22.0 |
| 50 | SG | 2.09 | 57.6 | 60.5 | 68.5 | -37.3 | -34.4 | -32.5 | -65.8 | -67.8 | -72.5 | 35.6 | 27.5 | 31.0 |

*SG, strain gage.

(b) SI Units

| $S_{max}$, MN/m² | Experimental method (*) | $K_{el}$ | Maximum local stress, MN/m² | | | Half-cycle residual stress, MN/m² | | | Minimum local stress, MN/m² | | | Full-cycle residual stress, MN/m² | | |
|---|---|---|---|---|---|---|---|---|---|---|---|---|---|---|
| | | | First cycle | | Stabilized | First cycle | | Stabilized | First cycle | | Stabilized | First cycle | | Stabilized |
| | | | Experimental | Calculated | | Experimental | Calculated | | Experimental | Calculated | | Experimental | Calculated | |
| 172 | SG | 2.16 | 361 | 351 | 369 | -10.3 | -10.3 | 0 | -308 | -307 | -313 | 70.3 | 55.1 | 63.4 |
| 207 | SG | 2.12 | 354 | 360 | 386 | -88.2 | -74.4 | -51.7 | -342 | -351 | -376 | 107 | 82.7 | 68.9 |
| 241 | SG | 2.15 | 364 | 368 | 420 | -147 | -135 | -86.1 | -371 | -382 | -410 | 144 | 121 | 103 |
| 276 | SG | 2.12 | 371 | 382 | 438 | -192 | -183 | -141 | -399 | -406 | -448 | 176 | 158 | 138 |
| 310 | SG | 2.17 | 391 | 398 | 444 | -235 | -222 | -200 | -431 | -439 | -469 | 222 | 181 | 152 |
| 344 | SG | 2.09 | 397 | 417 | 472 | -257 | -237 | -224 | -453 | -467 | -500 | 245 | 189 | 214 |

*SG, strain gage.

21

# TABLE III.- ESTIMATES OF FATIGUE LIFE

$$\left[ K_T = 2;\ 2024\text{-}T3 \text{ aluminum alloy} \right]$$

| $S_{max}$ | | R | Observed life, cycles (a) | Estimated life, cycles |
|---|---|---|---|---|
| ksi | MN/m$^2$ | | | |
| 25 | 172 | 0 | 190 000 | [b]72 500 |
| 30 | 207 | 0 | 83 000 | [b]45 700 |
| 35 | 241 | 0 | 46 000 | [b]30 900 |
| 40 | 276 | 0 | 27 500 | [b]24 000 |
| 45 | 310 | 0 | 16 500 | [b]17 000 |
| 50 | 344 | 0 | 10 500 | [b]13 700 |
| 25 | 172 | -1 | 19 500 | [c]10 000 |
| 30 | 207 | -1 | 7 300 | [c]5 000 |
| 35 | 241 | -1 | 2 750 | [c]2 000 |
| 40 | 276 | -1 | 1 400 | [c]1 000 |
| 45 | 310 | -1 | 630 | [c]600 |
| 50 | 344 | -1 | 270 | [c]200 |

[a]Observed lives taken from references 5 and 6.

[b]Estimates based on data for unnotched specimens from reference 4.

[c]Estimates based on data for unnotched specimens from reference 5.

# NASA SCIENTIFIC AND TECHNICAL PUBLICATIONS

**TECHNICAL REPORTS:** Scientific and technical information considered important, complete, and a lasting contribution to existing knowledge.

**TECHNICAL NOTES:** Information less broad in scope but nevertheless of importance as a contribution to existing knowledge.

**TECHNICAL MEMORANDUMS:** Information receiving limited distribution because of preliminary data, security classification, or other reasons.

**CONTRACTOR REPORTS:** Technical information generated in connection with a NASA contract or grant and released under NASA auspices.

**TECHNICAL TRANSLATIONS:** Information published in a foreign language considered to merit NASA distribution in English.

**TECHNICAL REPRINTS:** Information derived from NASA activities and initially published in the form of journal articles.

**SPECIAL PUBLICATIONS:** Information derived from or of value to NASA activities but not necessarily reporting the results of individual NASA-programmed scientific efforts. Publications include conference proceedings, monographs, data compilations, handbooks, sourcebooks, and special bibliographies.

*Details on the availability of these publications may be obtained from:*

## SCIENTIFIC AND TECHNICAL INFORMATION DIVISION

# NATIONAL AERONAUTICS AND SPACE ADMINISTRATION

Washington, D.C. 20546